Application of Adaptive Integral Method to Scattering Analysis of Arbitrarily Shaped Radomes

Wei-Jiang Zhao[1,2], Le-Wei Li[2,3], and Yeow-Beng Gan[1]
[1]Temasek Laboratories
National University of Singapore, Kent Ridge, Singapore 119260
[2]Department of Electrical and Computer Engineering
National University of Singapore, Kent Ridge, Singapore 119260
[3]High Performance Computations for Engineered Systems Programme
Singapore-MIT Alliance, Kent Ridge, Singapore 119260
tslzwj@nus.edu.sg, lwli@nus.edu.sg, and tslganyb@nus.edu.sg

I. Introduction

A radome is a dielectric shell used to protect its radar system from a variety of environmental effects and usually takes different shapes in actual applications. Approximation methods for treating the propagation through a radome include high frequency methods such as ray tracing technique or its modified variations. An important assumption in high frequency methods is that the structures have smooth surfaces and electrically large radius of curvature. For some radome types with sharp tips, such as airbone radomes, the high frequency approximation becomes less accurate, and hence no longer valid. Clearly, a more accurate approach is to employ a computationally rigorous analysis, such as the method of moments (MoM). However, due to the traditional $O(N^2)$ storage and $O(N^3)$ CPU time requirements, the MoM can only be used for electrically small radome structures. Recently, several fast integral algorithms have been developed to reduce memory and complexity without appreciable compromise in accuracy. One of the most powerful methods is the adaptive integral method (AIM) developed by Bleszynski *et al*. [1], and has been successfully applied to the analysis of scattering by, and radiation in, very complex structures. For surface scatterers, AIM has $O(N^{1.5}\log N)$ computational complexity and $O(N^{1.5})$ memory requirements. In this paper, the AIM is extended to the analysis of scattering by radomes of arbitrary shape. The method can be applied to efficiently and accurately analyze dielectric radomes of sizes much larger than those handled using direct numerical methods. And it also provides solution accuracy higher than that in a high frequency method, in general.

II. Formulations

The problem of plane wave scattering by a dielectric shell is considered in [2]. Considered an arbitrarily shaped dielectric shell characterized by a permittivity ε_2 and a permeability μ_2, and immersed in a homogeneous medium having parameters of a permittivity ε_1 and a permeability μ_1. S_o and S_i denote the outer and the inner surfaces of the shell respectively, while $\boldsymbol{E}^i$ and $\boldsymbol{H}^i$ stand for the incident electric and magnetic fields, respectively. By introducing equivalent electric current $\boldsymbol{J}_o$ and magnetic current $\boldsymbol{M}_o$ on the outer surface and equivalent electric current $\boldsymbol{J}_i$ and magnetic current $\boldsymbol{M}_i$ on the inner surface of the shell, and enforcing the boundary conditions of the fields on the surfaces, one has combined field formulations for the above four unknown surface currents [2]:

$$\left[\boldsymbol{E}_1^s(\boldsymbol{J}_o, \boldsymbol{M}_o) + \boldsymbol{E}_2^s(\boldsymbol{J}_o, \boldsymbol{M}_o) + \boldsymbol{E}_2^s(\boldsymbol{J}_i, \boldsymbol{M}_i)\right]_{\tan} = -\boldsymbol{E}^i\big|_{\tan}, \text{ on } S_o \tag{1a}$$

$$\left[\boldsymbol{H}_1^s(\boldsymbol{J}_o, \boldsymbol{M}_o) + \boldsymbol{H}_2^s(\boldsymbol{J}_o, \boldsymbol{M}_o) + \boldsymbol{H}_2^s(\boldsymbol{J}_i, \boldsymbol{M}_i)\right]_{\tan} = -\boldsymbol{H}^i\big|_{\tan}, \text{ on } S_o \tag{1b}$$

$$\left[\boldsymbol{E}_2^s(\boldsymbol{J}_o, \boldsymbol{M}_o) + \boldsymbol{E}_1^s(\boldsymbol{J}_i, \boldsymbol{M}_i) + \boldsymbol{E}_2^s(\boldsymbol{J}_i, \boldsymbol{M}_i)\right]_{\tan} = 0, \text{ on } S_i \tag{1c}$$

$$\left[\boldsymbol{H}_2^s(\boldsymbol{J}_o, \boldsymbol{M}_o) + \boldsymbol{H}_1^s(\boldsymbol{J}_i, \boldsymbol{M}_i) + \boldsymbol{H}_2^s(\boldsymbol{J}_i, \boldsymbol{M}_i)\right]_{\tan} = 0, \text{ on } S_i \ . \tag{1d}$$

The superscript 's' denotes scattered fields, and the subscript denotes the medium in which the scattered fields are evaluated. The expressions of scattered fields are given by [3]

$$\boldsymbol{E}_i^s(\boldsymbol{r}) = j\omega \boldsymbol{A}_i(\boldsymbol{r}) + \nabla V_i(\boldsymbol{r}) + \nabla \times \frac{\boldsymbol{F}_i(\boldsymbol{r})}{\varepsilon_i} \tag{2a}$$

$$\boldsymbol{H}_i^s(\boldsymbol{r}) = j\omega \boldsymbol{F}_i(\boldsymbol{r}) + \nabla U_i(\boldsymbol{r}) + \nabla \times \frac{\boldsymbol{A}_i(\boldsymbol{r})}{\varepsilon_i}. \tag{2b}$$

The various vector potentials and scalar potentials are given by

$$\boldsymbol{A}_i(\boldsymbol{r}) = \frac{\mu_i}{4\pi} \iint_S \boldsymbol{J}(\boldsymbol{r}') G_i(\boldsymbol{r}, \boldsymbol{r}') dS(\boldsymbol{r}') \tag{3a}$$

$$\boldsymbol{F}_i(\boldsymbol{r}) = \frac{\varepsilon_i}{4\pi} \iint_S \boldsymbol{M}(\boldsymbol{r}') G_i(\boldsymbol{r}, \boldsymbol{r}') dS(\boldsymbol{r}') \tag{3b}$$

$$V_i(\boldsymbol{r}) = -\frac{1}{4\pi j\varpi \varepsilon_i} \iint_S \nabla_s' \cdot \boldsymbol{J}(\boldsymbol{r}') G_i(\boldsymbol{r}, \boldsymbol{r}') dS(\boldsymbol{r}') \tag{3c}$$

$$U_i(\boldsymbol{r}) = -\frac{1}{4\pi j\varpi \mu_i} \iint_S \nabla_s' \cdot \boldsymbol{M}(\boldsymbol{r}') G_i(\boldsymbol{r}, \boldsymbol{r}') dS(\boldsymbol{r}') \tag{3d}$$

where S denotes the surface of the shell, and $G_i(\mathbf{r}, \mathbf{r}')$ is the Green's function. Equations (1a)-(1d) can be discretized by first expanding $\mathbf{J}_o$, $\mathbf{M}_o$, $\mathbf{J}_i$ and $\mathbf{M}_i$ as

$$\boldsymbol{J}_o(\boldsymbol{r}') = \sum_{n=1}^{N_o} \boldsymbol{I}_{on} \boldsymbol{f}_n(\boldsymbol{r}'),\ \boldsymbol{M}_o(\boldsymbol{r}') = \sum_{n=1}^{N_o} \boldsymbol{M}_{on} \boldsymbol{f}_n(\boldsymbol{r}'),\ \boldsymbol{J}_i(\boldsymbol{r}') = \sum_{n=1}^{N_i} \boldsymbol{I}_{in} \boldsymbol{f}_n(\boldsymbol{r}'),\ \boldsymbol{M}_i(\boldsymbol{r}') = \sum_{n=1}^{N_i} \boldsymbol{M}_{in} \boldsymbol{f}_n(\boldsymbol{r}') \tag{4}$$

where N_o and N_i represents the total numbers of edges on S_o and S_i, respectively, and $\mathbf{f}_n(\mathbf{r})$ represents the Rao-Wilton-Glisson (RWG) vector basis functions [4]. Substituting (4) into (1a)-(1d) and applying Galerkin's method, we obtain a partitioned matrix equation

$$\begin{bmatrix} [Z_{mn}^{J_oJ_o}] & [C_{mn}^{J_oM_o}] & [Z_{mn}^{J_oJ_i}] & [C_{mn}^{J_oM_i}] \\ [D_{mn}^{M_oJ_o}] & [Y_{mn}^{M_oM_o}] & [D_{mn}^{M_oJ_i}] & [Y_{mn}^{M_oM_i}] \\ [Z_{mn}^{J_iJ_o}] & [C_{mn}^{J_iM_o}] & [Z_{mn}^{J_iJ_i}] & [C_{mn}^{J_iM_i}] \\ [D_{mn}^{M_iJ_o}] & [Y_{mn}^{M_iM_o}] & [D_{mn}^{M_iJ_i}] & [Y_{mn}^{M_iM_i}] \end{bmatrix} \begin{bmatrix} [I_{on}] \\ [M_{on}] \\ [I_{in}] \\ [M_{in}] \end{bmatrix} = \begin{bmatrix} [V_{om}] \\ [H_{om}] \\ [V_{im}] \\ [H_{im}] \end{bmatrix}. \tag{5}$$

Elements of impedance matrix in (5) can be expressed as the following forms:

$$Z_{mn}^{JJ} = \frac{jwm_i}{4p} \iint_{T_m} \mathbf{f}_m(\mathbf{r}) \cdot \mathbf{A}_{imn}(\mathbf{r}) dS(\mathbf{r}) + \frac{1}{j4pwe_i} \iint_{T_m} \nabla \cdot \mathbf{f}_m(\mathbf{r}) \cdot \Phi_{imn}(\mathbf{r}) dS(\mathbf{r}) \tag{6a}$$

$$Y_{mn}^{MM} = \frac{jwe_i}{4p} \iint_{T_m} \mathbf{f}_m(\mathbf{r}) \cdot \mathbf{A}_{imn}(\mathbf{r}) dS(\mathbf{r}) + \frac{1}{j4pwm_i} \iint_{T_m} \nabla \cdot \mathbf{f}_m(\mathbf{r}) \cdot \Phi_{imn}(\mathbf{r}) dS(\mathbf{r}) \tag{6b}$$

$$C_{mn}^{JM} = \frac{1}{4p} \iint_{T_m} \nabla \times \mathbf{f}_m(\mathbf{r}) \cdot \mathbf{A}_{imn}(\mathbf{r}) dS(\mathbf{r}) \tag{6c}$$

$$D_{mn}^{MJ} = -C_{mn}^{JM} \tag{6d}$$

where

$$\mathbf{A}_{imn}(\mathbf{r}) = \iint_{T_n} \mathbf{f}_n(\mathbf{r}') G_i(\mathbf{r}, \mathbf{r}') d\mathbf{r}' \tag{7a}$$

$$\Phi_{imn}(\mathbf{r}) = \iint_{T_n} \nabla \cdot \mathbf{f}_n(\mathbf{r}') G_i(\mathbf{r}, \mathbf{r}') d\mathbf{r}'. \tag{7b}$$

To apply the AIM, we first enclose the whole object in a rectangular region and recursively subdivide it into small rectangular cells. Then we translate the original triangular basis functions to rectangular grids to permit the use of FFT to perform the matrix-vector multiplication. $\mathbf{f}_m(\mathbf{r})$, $\nabla \cdot \mathbf{f}_m(\mathbf{r})$ and $\nabla \times \mathbf{f}_m(\mathbf{r})$ can be approximated as a combination of the Dirac delta functions on the rectangular grids

$$\mathbf{f}_m(\mathbf{r}) \approx \sum_{q=1}^{(M+1)^3} (\Lambda_{mq}^x \hat{\mathbf{x}} + \Lambda_{mq}^y \hat{\mathbf{y}} + \Lambda_{mq}^z \hat{\mathbf{z}}) d(\mathbf{r} - \mathbf{r}_{mq}) \tag{8a}$$

$$\nabla \cdot \mathbf{f}_m \approx \sum_{q=1}^{(M+1)^3} \Lambda_{mq} d(\mathbf{r} - \mathbf{r}_{mq}) . \tag{8b}$$

$$\nabla \times f_m(r) \approx \sum_{q=1}^{(M+1)^3} (\Lambda_{c,mq}^x \hat{\mathbf{x}} + \Lambda_{c,mq}^y \hat{\mathbf{y}} + \Lambda_{c,mq}^z \hat{\mathbf{z}}) d(\mathbf{r} - \mathbf{r}_{mq}) . \tag{8c}$$

where M is the expansion order, $(\Lambda_{mq}^x , \Lambda_{mq}^y , \Lambda_{mq}^z)$, Λ_{mq}, and $(\Lambda_{c,mq}^x , \Lambda_{c,mq}^y , \Lambda_{c,mq}^z)$ are the expansion coefficients, $d(\mathbf{r} - \mathbf{r}_{mq})$ is the Dirac function, and $\mathbf{r}_{mq}$ is the point on the grid surrounding the *m*th edge. Once we find this translation, we can approximate the elements of impedance matrix in (5) as

$$Z_{mn}^{JJ} \approx \frac{jwm_i}{4p} \sum_{k=1}^{3} \sum_{u=1}^{(M+1)^3} \sum_{v=1}^{(M+1)^3} \Lambda_{mu}^k G(\mathbf{r}_u, \mathbf{r}_v') \Lambda_{nv}^k + \frac{1}{j4pwe_i} \sum_{u=1}^{(M+1)^3} \sum_{v=1}^{(M+1)^3} \Lambda_{mu} G(\mathbf{r}_u, \mathbf{r}_v') \Lambda_{nv} \tag{9a}$$

$$Y_{mn}^{JJ} \approx \frac{jwe_i}{4p} \sum_{k=1}^{3} \sum_{u=1}^{(M+1)^3} \sum_{v=1}^{(M+1)^3} \Lambda_{mu}^k G(\mathbf{r}_u, \mathbf{r}_v') \Lambda_{nv}^k + \frac{1}{j4pwm_i} \sum_{u=1}^{(M+1)^3} \sum_{v=1}^{(M+1)^3} \Lambda_{mu} G(\mathbf{r}_u, \mathbf{r}_v') \Lambda_{nv} \tag{9b}$$

$$C_{mn}^{JM} \approx \frac{1}{4p} \sum_{k=1}^{3} \sum_{u=1}^{(M+1)^3} \sum_{v=1}^{(M+1)^3} \Lambda_{c,mu}^k G(\mathbf{r}_u, \mathbf{r}_v') \Lambda_{nv}^k . \tag{9c}$$

By employing the multipole moments approximation [1], the translation of (8a)-(8c) can be accomplished and the expansion coefficients can be obtained. Expansion coefficients $(\Lambda_{mq}^x, \Lambda_{mq}^y, \Lambda_{mq}^z)$ and Λ_{mq} can be obtained by computing multipole expansions of basis function $\mathbf{f}_m(\mathbf{r})$ and divergence of basis function $\nabla \cdot \mathbf{f}_m(\mathbf{r})$, respectively. This is well known in the implementation of AIM solution for perfectly electrically conducting (PEC) scatterers. In order to obtain expansion coefficients $(\Lambda_{c,mq}^x, \Lambda_{c,mq}^y, \Lambda_{c,mq}^z)$, one needs to compute multipole expansions of the curl of basis function $\nabla \times \mathbf{f}_m(\mathbf{r})$. Actually, the computation of multipole moments of the curl of basis functions can be incorporated into the computation of multipole moments of basis functions [1].

The impedance matrix in (5) is then decomposed into the near interaction component A^{near} and far interaction component A^{far}. A^{near} can be computed as the difference between Z_{mn}^{JJ}, Y_{mn}^{MM}, and C_{mn}^{JM} in (6a)-(6c) and those in (9a)-(9c). Since a given basis function has only a limited number of nearby testing functions, A^{near} is a sparse matrix. A^{far} can be computed using (9a)-(9c).

The matrix *G* in the above formulations is Toeplitz, and this enables the use of FFT to accelerate the computation of the matrix-vector multiplication. Therefore the algorithm is less memory and CPU time demanding.

We note that from (9a)-(9c), one has to make FFT computation only when the multiplication of far interaction component of Z_{mn}^{JJ}, Y_{mn}^{MM} and current vector are computed, and the FFT results can be exploited and no extra FFT operations is needed when the multiplication of far interaction component of C_{mn}^{JM} and current vector is computed.

III. Numerical results

To demonstrate applicability of the above formulation and to validate our computer codes, scattering by a spherical dielectric shell located in free space is first considered. The shell has an inner radius of $0.5\,l$ and an outer radius $0.6\,l$, and a relative permittivity $e_r = 4$. Fig. 1 depicts the computed bistatic radar cross section s_{qq} for the dielectric shell, when the number of unknowns is 5052, the AIM grid spacing is $0.08\,l$, the expansion order is 3, and elements further than $0.3\,l$ apart were considered as far interactions. The numerical results are compared with those exact data and an excellent agreement is observed.

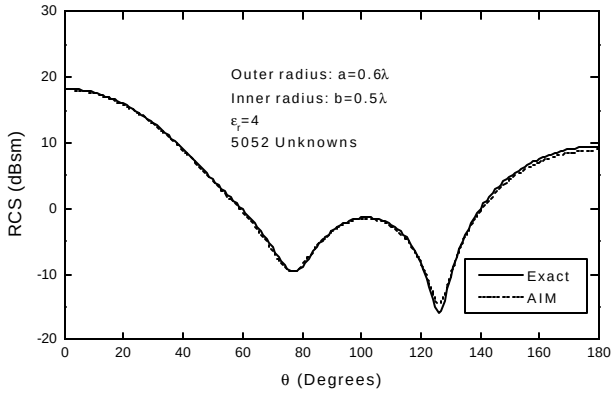

Fig. 1. The bistatic RCS s_{qq} of a dielectric spherical shell of inner radius *a*, and outer radius *b*. The shell is centered at the origin.

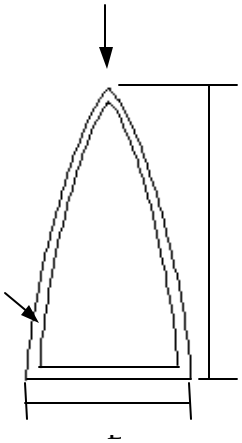

Fig.2. Von Karman radome geometry

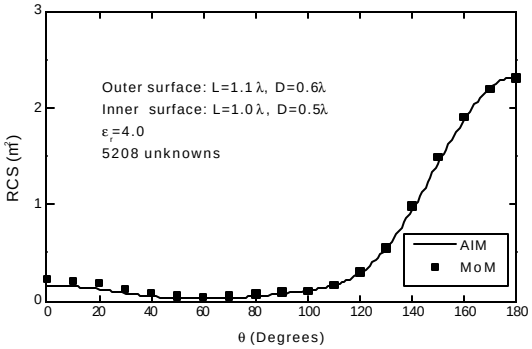

Fig.3. The bistatic RCS s_{qq} of the radome

As the second test case, we consider the scattering by a Von Karman radome whose geometry is shown in Fig. 2. *D* is the base diameter and *L* is the length of the radome. Fig. 3 shows the bistatic RCS of the radome, when the number of unknowns is 5208, the grid spacing is $0.08\,l$, the expansion order is 3, and elements further than $0.3\,l$ apart were considered as far interactions. Also shown in this figure is the comparison with the MoM data [2]. As seen, a very good agreement between the AIM and MoM data is found, which again shows our fairly accurate and fast prediction.

IV. Conclusions

A fast algorithm based on the adaptive integral method (AIM) is described for the analysis of scattering by a dielectric radome of arbitrary shape. The application of AIM significantly reduces the memory and CPU time requirement for solving the integral equation, and hence the algorithm presented in this paper can be applied to problems with electrically large sized radomes, and provides solution-accuracy much higher than those of high frequency methods.

References

[1] E. Bleszynski, M. Bleszynski, and T. Jaroszewicz, AIM: Adaptive integral method for solving large-scale electromagnetic scattering and radiation problems, Radio Sci, 31 (1996), 1225-1251.

[2] E. Arvas and S. Ponnapalli, Scattering cross section of a small radome of arbitrary shape, IEEE Trans Antennas Propagat, 37 (1989), 655-658.

[3] K. Umashankar, A. Taflove, and S. M. Rao, Electromagnetic scattering by arbitrary shaped three-dimensional homogeneous lossy dielectric objects, IEEE Trans Antennas Propagat, 34 (1986), 758-766.

[4] S. M. Rao, D. R. Wilton, and A. W. Glisson, Electromagnetic scattering by surfaces of arbitrary shape, IEEE Trans Antennas Propagat, 30 (1982), 409-418.